Infrared Spectra of Zn and Cd Hydride Molecules and Solids

Xuefeng Wang and Lester Andrews*

Department of Chemistry, University of Virginia, McCormick Road, P. O. Box 400319, Charlottesville, Virginia 22904-4319

Received: August 10, 2004; In Final Form: September 22, 2004

Laser-ablated Zn and Cd atoms react with molecular hydrogens upon condensation at 4.5 K to form the metal dihydride molecules in solid hydrogen and neon. Ultraviolet irradiation increases these absorptions by an order of magnitude. Natural zinc- and cadmium isotopic splittings are resolved in solid *p*-H_2, *o*-D_2, and HD. Weaker absorptions are assigned to the linear HMMH molecules and to metal cluster monohydrides with the assistance of DFT calculations. Upon sublimation of the hydrogen or neon matrix, the metal dihydride molecules polymerize into solid hydrides with broad absorption bands characteristic of hydrogen-bridge bonding.

Introduction

Zinc forms a hydrogen-bridged solid that decomposes into the elements in the 90−115 °C range, depending on the method of preparation.[1−4] A broad-band infrared spectrum of the solid has been described,[3] and the optical absorption and dielectric properties have been measured.[5] The typical preparation involves ZnI_2 and $LiAlH_4$, and it is difficult to obtain a pure ZnH_2 product. We report here a preparation of solid zinc hydride from the pure elements.

The ZnH_2 molecule was first observed after UV irradiation of Zn atoms and H_2 in excess argon or krypton and later by reaction of Zn* from a microwave discharge with H_2 in argon.[6,7] Both studies observed antisymmetric stretching and bending modes for the linear ZnH_2 molecule.

Cadmium hydride is much less stable,[1,4,8] decomposing above −20 °C, and accordingly, solid CdH_2 has received less investigation. The linear CdH_2 molecule has been characterized following reaction of Cd* from a discharge with H_2 and capture in solid argon.[7]

We report here an investigation of Zn and Cd hydrides in solid molecular hydrogens. After evaporation of the solid hydrogen host matrix, pure solid ZnH_2 and CdH_2 remain for infrared analysis. Similar methods have been employed to record infrared spectra of solid aluminum, indium, and magnesium hydrides.[9−13] The $J = 0$ solids (*p*-H_2, *o*-D_2, HD) allow for the resolution of natural zinc isotopes for further characterization of the linear ZnH_2 and HZnZnH molecules.

Experimental and Computational Methods

The experiments for reactions of laser-ablated metal atoms with hydrogen during condensation in excess hydrogen and neon have been described in detail previously.[14,15] The Nd:YAG laser fundamental (1064 nm, 10 Hz repetition rate with 10 ns pulse width) was focused onto a rotating zinc (Alfa Inorganics) or a cadmium (Fisher) metal target. The laser energy was varied from 5 to 20 mJ/pulse. Laser-ablated metal atoms were codeposited with hydrogen (0.2−4%) in excess neon or pure hydrogen onto a 4.5 K CsI cryogenic window at 2−4 mmol/h (H_2/Ne for 1 h and pure H_2 for 30 min). Isotopic D_2 and HD (Cambridge Isotopic Laboratories) and selected mixtures were used in different experiments. FTIR spectra were recorded at 0.5 cm^{-1} resolution with 0.1 cm^{-1} accuracy or 0.13 cm^{-1} resolution with 0.02 cm^{-1} accuracy on a Nicolet 750 using an HgCdTe detector. Matrix samples were annealed at different temperatures, and selected samples were subjected to broadband photolysis by a medium-pressure mercury arc lamp (Philips, 175 W) with globe removed or by ArF eximer laser (193 nm) irradiation (Optex). A simple and efficient converter[16] was used to prepare para hydrogen and ortho deuterium[17,18] samples for similar experiments.

Density functional theoretical calculations of zinc and cadmium hydrides are given for comparison. The Gaussian 98 program[19] was employed to calculate the structures and frequencies of expected molecules using the B3LYP functional. The 6-311++G(3df,3pd) basis set for both Zn and H atoms and SDD pseudopotential for Cd were used. All the geometrical parameters were fully optimized, and the harmonic vibrational frequencies were obtained analytically at the optimized structures.

Results

Infrared spectra are presented for laser-ablated Zn and Cd reactions with H_2, D_2, and HD in the pure solids and in excess neon. Common absorptions assigned previously to $H^-(H_2)_n$ and $H(H_2)_n$ will not be discussed.[20,21] Calculations of product molecules are given to assist identification.

Infrared Spectra. Figure 1 compares infrared spectra for laser-ablated Zn and Cd reactions with normal hydrogen, and the product absorptions are listed in Tables 1 and 2. The major products with zinc are ZnH_2 (1880.6 cm^{-1}), the ZnZnH species at 1647.9 cm^{-1}, and ZnH (1498.5 cm^{-1}) based on comparison with previous argon matrix spectra.[7] The corresponding cadmium products are observed to be 116−165 cm^{-1} lower. Note that both metal monohydrides and the new species increase 25% on $\lambda > 470$ nm irradiation, whereas the metal dihydrides require UV light for growth. Similar spectra observed for both metals in normal deuterium are given in Figure 2. The major products are ZnD_2 (1361.6 cm^{-1}), ZnZnD (1194.4 cm^{-1}), and ZnD (1091.1 cm^{-1}). The analogous cadmium products are 91−117 cm^{-1} lower.

* Author for correspondence. E-mail: lsa@virginia.edu.

10.1021/jp046414m CCC: $27.50
Published on Web 11/18/2004

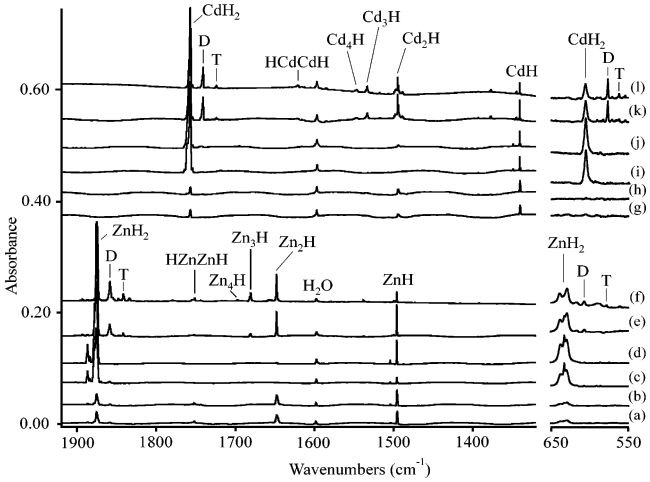

Figure 1. Infrared spectra in the 1920−1320 and 660−560 cm^{-1} regions for laser-ablated Zn and Cd codeposited with normal hydrogen at 4.5 K. (a) Zn and H_2 (2 mmol) deposited, (b) after $\lambda > 470$ nm irradiation for 15 min, (c) after 240−380 nm irradiation for 15 min, (d) after 193 nm irradiation (4 mJ/pulse, 10 Hz) for 5 min, (e) after annealing to 6.3 K, and (f) after annealing to 7.0 K. (g) Cd and H_2 (2 mmol) deposited, (h) after $\lambda > 470$ nm irradiation for 15 min, (i) after 240−380 nm irradiation for 15 min, (j) after 193 nm irradiation (4 mJ/pulse, 10 Hz) for 5 min, (k) after annealing to 6.4 K, and (l) after annealing to 6.7 K. (D: dimer, T: trimer)

TABLE 1: Infrared Absorptions (cm^{-1}) for Zinc Hydrides in Solid Hydrogen and Neon

$Ne(H_2)$	$Ne(D_2)$	n-H_2	p-H_2	n-D_2	o-D_2	HD	ident.
		4143 sh	4143.1	2977.1	2977.2	3614.8	$ZnH_2(H_2)_n$
		4133.6	−	2973.3			
1966.2	1417.0	1963.2	1965.8	1415.7	1417.1	1965.1, 1416.7	HZnOH
1898.5		1887.0	1891.1	1372.0	−		(X)ZnH_2
1880.6	1362.6	1875.5	1880.5	1361.5	1363.0	1878.7,[a] 1352.6	ZnH_2
1867.2	1352.0	1858.9	1863.8	1348.4	1350.7	1861.0, 1340.9	$(ZnH_2)_2$
1845.6	1338	1842.0	1842.9	1328.4	1329.0	1843.8	$(ZnH_2)_3$
1746.8		1752.2	1752.2	1255.5	1259.5	1763.3,[b] 1270.9	HZnZnH
		1697.2					Zn_4H
1682.6		1680.8	1681.9	1214.0	−	1681.4, 1215.7	Zn_3H
1647.8	1194.0	1647.9	1648.5	1194.4	1195.6	1649.4, 1194.7	ZnZnH
1498.5	1091.3	1495.4	1496.1	1091.1	1091.6	1496.6, 1090.1	ZnH
632.5	456.4	632.1	631.9	456.0	456.1	553.4	ZnH_2
608.2		606.6	606.8				$(ZnH_2)_2$

[a] ZnH_2, 1879.5 and 631.5 cm^{-1}; ZnD_2, 1363.9 and 457.8 cm^{-1}. [b] HZnZnH, 1749.8 cm^{-1}; DZnZnD, 1261.8 cm^{-1}.

TABLE 2: Infrared Absorptions (cm^{-1}) for Cadmium Hydrides in Solid Hydrogen and Neon

$Ne(H_2)$	$Ne(D_2)$	n-H_2	p-H_2	n-D_2	o-D_2	HD	ident.
		4134.0		2977.7		3615.0	$CdH_2(H_2)_n$
1764.1	1271.0	1762.5	1763.4	1270.1	1270.8	1765.3,[a] 1267.0[a]	CdH_2
		1758.1	1760.9	1269.3	1270.4		CdH_2 site
1751.0	1262.5	1741.9	1748.0	1257.5			$(CdH_2)_2$
1734.7	1251.1	1724.9		1242.4			$(CdH_3)_3$
1632.5	1169.5	1621.8		1166.5		1629.0, 1170.9	HCdCdH
		1547.2		1117.2		1549.4[b]	Cd_4H
1534.7	1107.3	1533.8		1108.6		1536.2[b]	Cd_3H
1493.0	1080.2	1494.8		1077.7		1488.2,[c] 1076.2	CdCdH
		1344.7	1344.7	981.7	979.0		CdH site
1340.8	977.5	1340.4	1340.4	978.7	978.7	1342.3, 977.0	CdH
604.6	435.6	605.1	604.5	435.4	435.4		CdH_2
604.0	434.5		603.7	434.3	434.3		CdH_2
584.0		576.6	582.2				$(CdH_2)_2$

[a] CdH_2, 1762.8 and 604.4, 603.1 cm^{-1}; CdD_2, 1271.3 and 435.8, 434.9 cm^{-1}. [b] D counterparts with HD at 1117.2 and 1108.3 cm^{-1}. [c] Site splitting at 1497.8 cm^{-1}.

Pure HD was employed as a reagent/matrix for Zn and Cd, and the spectra are illustrated in Figures 3 and 4. Note that ZnH and ZnD are 1.2 cm^{-1} higher and 1.0 cm^{-1} lower, respectively,

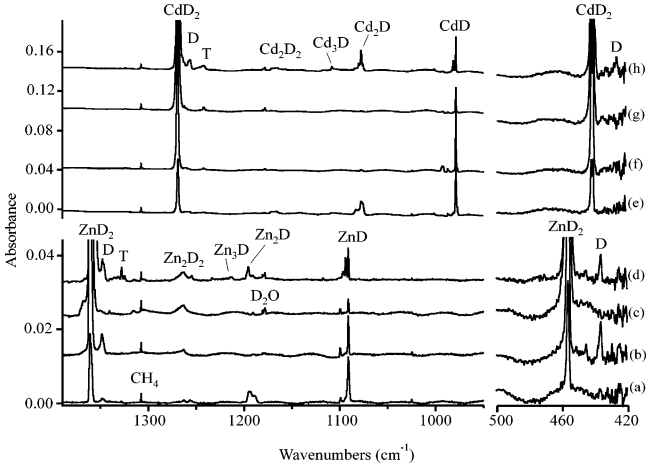

Figure 2. Infrared spectra in the 1390−950 and 500−420 regions for laser-ablated Zn codeposited with normal deuterium at 4.5 K. (a) Zn and D_2 (2 mmol) deposited, (b) after 240−380 nm irradiation for 15 min, (c) after $\lambda > 220$ nm irradiation for 15 min, and (d) after annealing to 9.5 K, (e) Cd and D_2 (2 mmol) deposited, (f) after 240−380 nm irradiation for 15 min, (g) after $\lambda > 220$ nm irradiation for 15 min, and (h) after annealing to 9.0 K. (D: dimer, T: trimer)

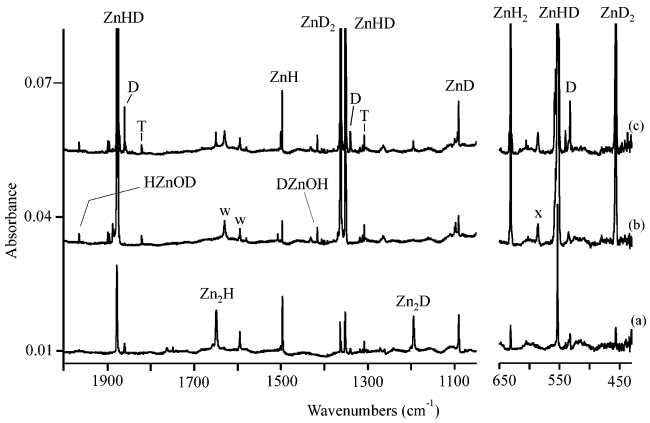

Figure 3. Infrared spectra in the 2000−1050 and 650−430 cm^{-1} regions for laser-ablated Zn codeposited with pure HD at 4.5 K. (a) Zn and HD (2 mmol) deposited for 30 min, (b) after $\lambda > 220$ nm irradiation for 15 min, and (c) after annealing to 7.2 K. The "x" denotes a 586 cm^{-1} band common to different metal experiments. The "w" denotes water.

in the solid HD medium, and that CdH and CdD are 1.9 cm^{-1} higher and 1.7 cm^{-1} lower, respectively, in solid HD than in n-H_2 and n-D_2. Note that ZnHD and CdHD exhibit both stretching fundamentals.

Neon was employed as a host for similar reactions with added H_2 and D_2. Spectra are compared in Figure 5 for zinc; most of the bands are blue-shifted 3−5 cm^{-1} in solid neon from solid n-H_2. Tables 1 and 2 give the observed product frequencies.

Solid samples remained on the cold window after evaporation of the neon or solid molecular hydrogen matrix. Figure 6 compares the broad bands observed for these solid samples; neon matrix samples gave the same but weaker broad bands, owing to the lower yield of dihydride product. Table 3 shows the zinc hydride solid absorption centered at 1440 ± 10 cm^{-1} remains unchanged at room temperature; the deuterium counterpart appeared at 1050 ± 10 cm^{-1}. With HD, two broad bands were observed at 1500 and 1080 cm^{-1}. The broad cadmium hydride counterpart band center was measured at 1340 ± 10 cm^{-1}, and this absorption disappeared as the sample support approached room temperature. The deuterium counterpart at 970 ± 10 cm^{-1} appeared in spectra recorded as the support warmed

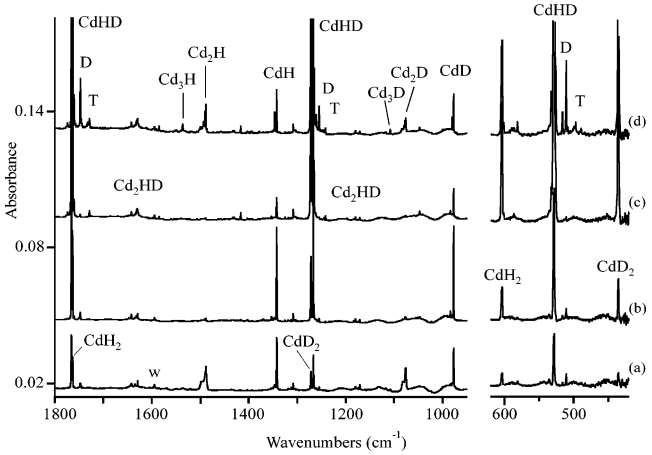

Figure 4. Infrared spectra in the 1800−950 and 620−420 cm^{-1} regions for laser-ablated Cd codeposited with pure HD at 4.5 K. (a) Cd and HD (2 mmol) deposited for 30 min, (b) after 240−380 irradiation for 15 min, (c) after $\lambda > 220$ nm irradiation for 15 min, and (d) after annealing to 7.7 K. The "w" denotes water.

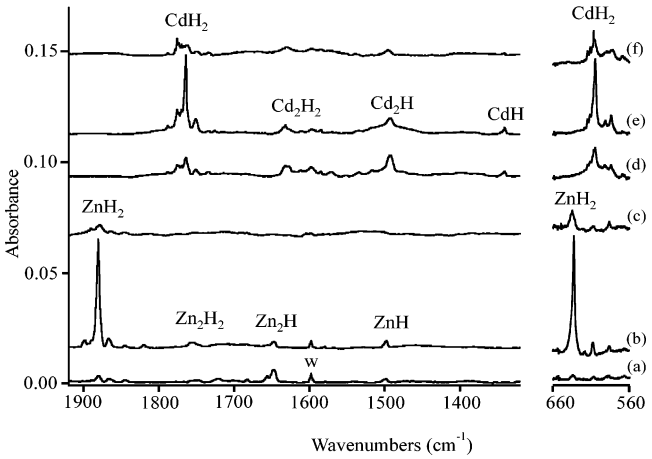

Figure 5. Infrared spectra in the 1920−1320 and 660−560 cm^{-1} regions for laser-ablated Zn and Cd codeposited with H_2 in excess neon at 4.5 K. (a) Zn and 10% H_2 in neon deposited, (b) after $\lambda > 220$ nm irradiation for 15 min, (c) after annealing to 10.5 K. (d) Cd and 8% H_2 in neon deposited, (e) after $\lambda > 220$ nm irradiation for 15 min, and (f) after annealing to 9.5 K. The "w" denotes water.

to 30−40 K, remained in spectra recorded from 200 to 230 K, decreased 50% in the 240−250 K range, and disappeared in the 260−280 K interval. Again, HD gave two broad bands that appeared at 1360 and 990 cm^{-1} for the cadmium hydride. These bands remained unchanged in spectra recorded up to 200 K, decreased in spectra taken at 230−250 K, and disappeared as the sample reached room temperature.

Table 4 gives values for samples of $J = 0$ solid molecular hydrogens (99% *p*-H_2 and *o*-D_2) that were also employed as reagent and matrix host since sharper infrared absorptions are typically observed.[22] The product bands were sharper and blue-shifted up to 5 cm^{-1} from the normal solid values. Natural metal isotopic splittings were resolved using 0.13 cm^{-1} resolution, and the best examples are illustrated in Figures 7, 8, and 9 for zinc, and Figure 10 for cadmium.

Calculations. The results of calculations for zinc and cadmium hydride molecules are presented in Tables 5 and 6. Our B3LYP bond lengths for the linear ZnH_2 and CdH_2 molecules are slightly longer than computed previously at the MP2 and CCSD levels,[7] and our computed frequencies are correspondingly lower and closer to the observed values.

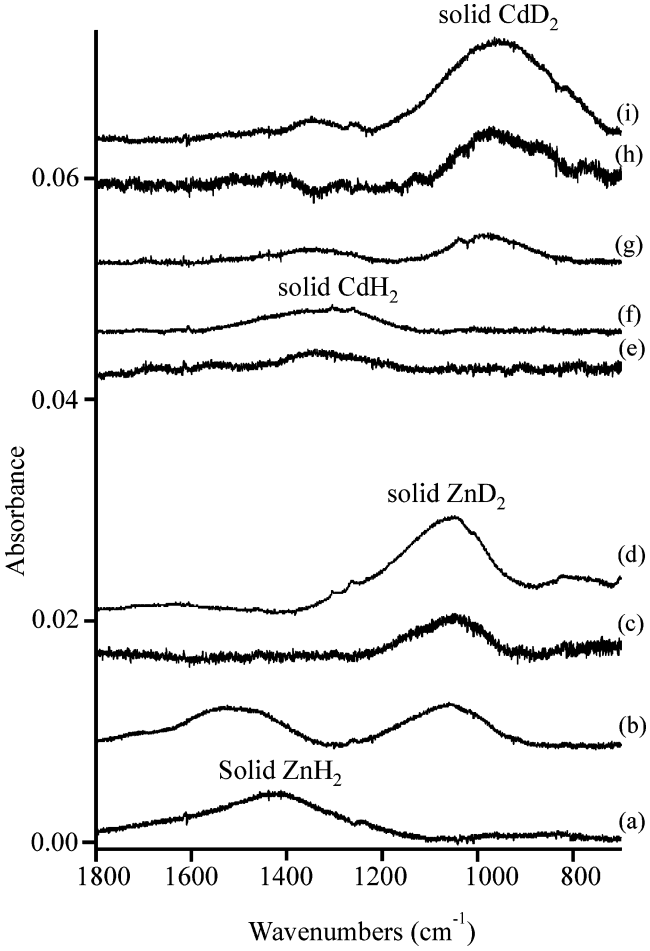

Figure 6. Broad absorptions observed from zinc and cadmium hydride samples after evaporating the matrix host. (a) Zn + 10% H_2 in neon, spectrum recorded at 30−90 K, (b) Zn + HD, spectrum recorded at 95−125 K, (c) Zn + 8% D_2 in neon, spectrum recorded at 30−60 K and amplified ×2, (d) Zn + D_2, spectrum recorded after annealing to 12 K, (e) Cd + 10% H_2 in neon, spectrum recorded at 60−90 K, (f) Cd + H_2, spectrum recorded after annealing to 12 K, (g) Cd + HD, spectrum recorded at 30−90 K, (h) Cd + 8% D_2 in neon, spectrum recorded at 30−90 K and amplified ×2, and (i) Cd + D_2, spectrum recorded at 30−60 K.

TABLE 3: Broad Infrared Absorption Bands (±10 cm^{-1}) Observed for Solid Metal Hydrides after Matrix Evaporation

	H_2	D_2	HD	H_2/D_2
Zn	1440 570	1050	1500 1080	1.37
Cd	1340	970	1360 990	1.38

Discussion

The zinc and cadmium hydride product assignments will be discussed in view of isotopic shifts, matrix shifts, and computed frequencies.

ZnH_2 and CdH_2. The major product molecules, linear ZnH_2 and CdH_2, are observed at 1875.5 and 1762.5 cm^{-1} in *n*-H_2, which are 5.3 and 4.6 cm^{-1} higher than argon matrix[7] values, respectively. These absorptions shift 5.0 and 0.9 cm^{-1} higher in *p*-H_2 and another 0.1 and 0.7 cm^{-1} higher, respectively, in solid neon. The computed B3LYP antisymmetric stretching frequencies of 1930.6 and 1807.3 cm^{-1} are just 55.1 and 45.2 cm^{-1} (2.9 and 2.6%) higher than the *n*-H_2 values. The degenerate bending modes observed at 632.5 and 604.6 cm^{-1} show

TABLE 4: Natural Metal Isotopic Frequencies (±0.02 cm^{-1}) Resolved for Zinc and Cadmium Hydrides in $J = 0$ Solid Matrix Samples

H_2	molecule	D_2	molecule	HD	molecule
1891.10	(X)$^{64}ZnH_2$			1879.46	$^{64}ZnH_2$
1890.36	(X)$^{66}ZnH_2$			1878.2	$^{64}ZnHD$
1889.68	(X)$^{68}ZnH_2$			1878.30	$^{66}ZnHD$
				1877.90	$^{68}ZnHD$
1880.50	$^{64}ZnH_2$	1362.96	$^{64}ZnD_2$	1363.93	$^{64}ZnD_2$
1879.68	$^{66}ZnH_2$	1361.78	$^{66}ZnD_2$	1362.74	$^{66}ZnD_2$
1879.28	$^{67}ZnH_2$	1361.22	$^{67}ZnD_2$	1362.18	$^{67}ZnD_2$
1878.90	$^{68}ZnH_2$	1360.67	$^{68}ZnD_2$	1361.63	$^{68}ZnD_2$
		1359.63	$^{70}ZnD_2$		
1863.85	$(^{64}ZnH_2)_2$	1350.72	$(^{64}ZnD_2)$	1352.65	$^{64}ZnHD$
1863.05	$(^{66}ZnH_2)_2$	1349.50	$(^{66}ZnD_2)$	1352.06	$^{66}ZnHD$
1862.27	$(^{68}ZnH_2)_2$	1348.41	$(^{68}ZnD_2)$	1351.52	$^{68}ZnHD$
1496.11	^{64}ZnH	1091.61	^{64}ZnD	1090.49	^{64}ZnD
1495.83	^{66}ZnH	1091.13	^{66}ZnD	1090.00	^{66}ZnD
1495.55	^{68}ZnH	1090.73	^{68}ZnD	1089.55	^{68}ZnD
1752.52	$^{64}Zn_2H_2$	1260.00	$^{64}Zn_2D_2$		
1752.30	$^{64}Zn^{66}ZnH_2$	1259.72	$^{64}Zn_2{}^{66}ZnD$		
1752.13[a]	$^{64}Zn^{68}ZnH_2$	1259.46[b]	$^{64}Zn^{68}ZnD_2$		
1751.98	$^{66}Zn^{68}ZnH_2$	1259.19	$^{66}Zn^{68}ZnD_2$		
1751.70	$^{68}Zn_2H_2$	1258.95	$^{68}ZnD_2$		
1763.62	$^{112}CdH_2$	1270.79	$^{112}CdD_2$		
1763.37	$^{114}CdH_2$	1270.43	$^{114}CdD_2$		

[a] Overlapped by $^{66}Zn_2H_2$. [b] Overlapped by $^{66}Zn_2D_2$.

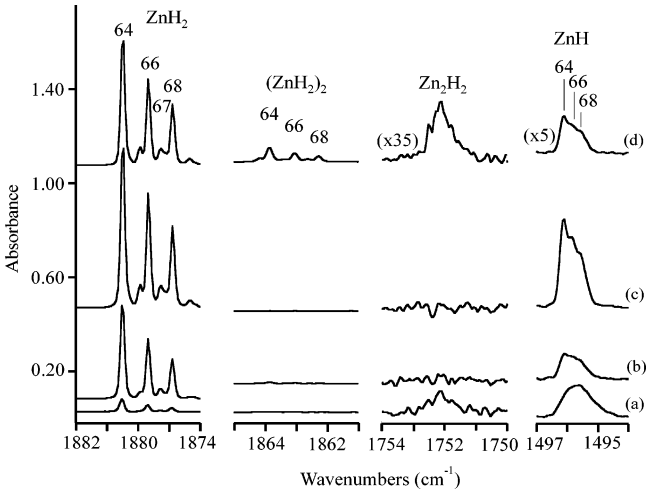

Figure 7. Infrared spectra (0.13 cm^{-1} resolution) in selected regions for laser-ablated Zn in *p*-H_2 at 4.5 K. (a) Zn and 99% *p*-H_2 (2 mmol), (b) after 240−380 nm irradiation for 15 min, (c) after 193 nm irradiation (4 mJ/pulse, 10 Hz) for 5 min, and (d) after annealing to 6.5 K.

evidence of splitting by the *n*-H_2 matrix and a slight (about 2 cm^{-1}) blue-shift from solid argon values.

Isotopic substitution confirms these assignments. First, the reactions with *n*-D_2 give strong new bands at 1361.5 and 1270.1 cm^{-1} (H/D ratios 1.3775 and 1.3851, respectively) with bending modes at 465.0 and 435.4 cm^{-1}. Second, similar reactions with HD give intermediate bending modes and both M−H and M−D stretching modes for the mixed isotopic molecules. Since the unobserved symmetric stretching modes are computed lower than the strong antisymmetric vibrations observed here, the M−H and M−D stretches if the MHD molecules fall below the strong observed bands. This is clear in the HD experiments (Figures 3 and 4) where small amounts of MH_2 and MD_2 isotopic molecules are observed as well. Third, the resolved natural metal isotopic splittings (Figures 7−10) demonstrate that a single metal atom is involved, and the metal isotopic shifts are precisely those computed for linear, centrosymmetric dihydride molecules.

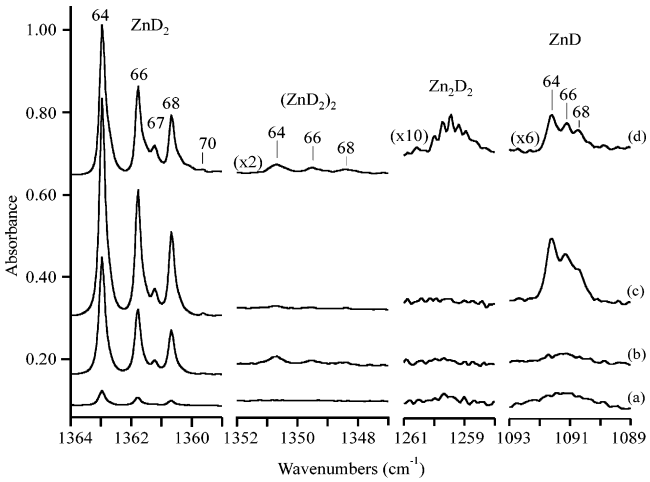

Figure 8. Infrared spectra (0.13 cm^{-1} resolution) in selected regions for laser-ablated Zn in *o*-D_2 at 4.5 K. (a) Zn and 99% *o*-H_2 (2 mmol), (b) after 240−380 nm irradiation for 15 min, (c) after 193 nm irradiation (4 mJ/pulse, 10 Hz) for 5 min, and (d) after annealing to 9.0 K.

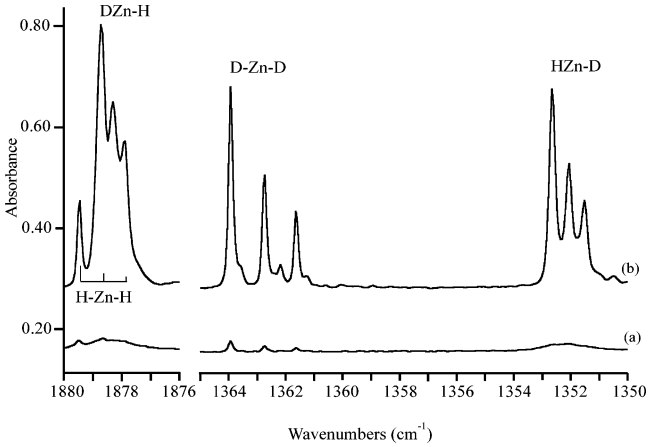

Figure 9. Infrared spectra (0.13 cm^{-1} resolution) in selected regions for laser-ablated Zn in pure HD at 4.5 K. (a) Zn and HD (2 mmol) deposited for 30 min, and (b) after $\lambda > 220$ nm irradiation for 15 min.

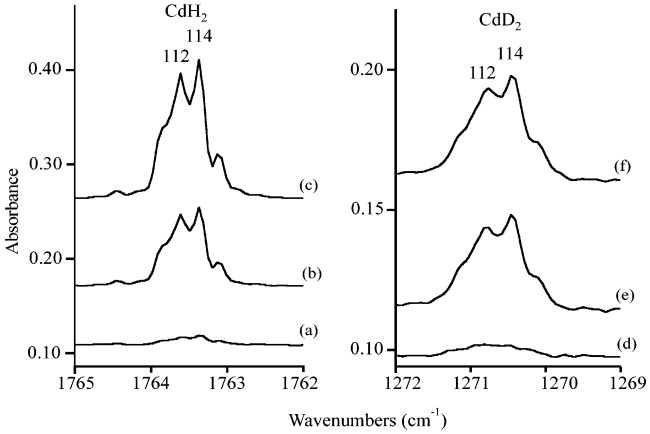

Figure 10. Infrared spectra (0.13 cm^{-1} resolution) in selected regions for laser-ablated Cd in *p*-H_2 at 4.5 K. (a) Cd and 99% *p*-H_2 (2 mmol), (b) after 240−380 nm irradiation for 15 min, and (c) after 193 nm irradiation (4 mJ/pulse, 10 Hz) for 5 min.

The zinc isotopic patterns for ZnH_2 in solid normal H_2 and for ZnD_2 in solid normal D_2 are not resolved because the bands are broadened by mixed para and ortho hydrogen molecules. However, the ZnH_2 isotopomers can be distinguished in solid para hydrogen and likewise for ZnD_2 in solid ortho deuterium. Natural zinc isotopes[23], three major (^{64}Zn, 48.6%; ^{66}Zn, 27.9%;

TABLE 5: Calculated Geometries, Vibrational Frequencies, and Intensities of Zinc Hydrides at the B3LYP/6-311++G(3df,3pd) Level of Theory

species	structure: Å	frequencies: cm^{-1}(intensities, km/mol)
ZnH ($^2\Sigma$)	ZnH: 1.622	^{64}ZnH: 1511.9(163); ^{64}ZnD: 1077.7(83)
Zn_2H ($^2\Sigma$)	ZnH: 1.597	Zn_2H: 1685.2(σ,587), 136.4(σ,0), 125.6(π,39 × 2)
linear	ZnZn: 2.653	Zn_2D: 1201.6(297), 135.8(0), 91.9(20 × 2)
Zn_3H ($^2A_1$)	ZnH: 1.594	Zn_3H: 1701.3(a_1,310), 174.1(b_2,2), 115.7(b_1,63), 105.7(a_1,1), 73.4(b_2,1), 23.2(a_1,0)
Planar C_{2v}	ZnZn′: 2.723	
	Zn′ZnZn′: 95.2	
Zn_4H	ZnH: 1.582	Zn_4H: 1739.1(a_1,266), 223.5(e,10 × 2),127.4(a_1,1), 78.2(e,0 × 2), 68.8(a_1,0), 58.8(e,0 × 2)
(C_{3v})	ZnZn′: 2.725	
	Zn′Zn′: 2.923	
ZnH_2 ($^1\Sigma_g^+$)	ZnH: 1.542	ZnH_2: 1929.9(σ_u, 328), 1917.8(σ_g, 0), 645.3(π_u, 152 × 2)
linear		ZnD_2: 1385.8(169), 1356.6(0), 463.4(78 × 2)
		ZnHD: 1924.0(169), 1371.1(80), 562.0(115 × 2)
Zn_2H_2 ($^1\Sigma_g^+$)	ZnH: 1.572	Zn_2H_2: 1845.7(σ_g,0), 1820.6(σ_u, 988), 421.1(πg,0 × 2), 328.3(π_u,103 × 2), 226.3(σ_g,0).
linear	ZnZn: 2.442	Zn_2D_2: 1315.7(0), 1297.8(502), 309.3(0 × 2), 234.0(52 × 2), 224.6(0)
		Zn_2HD: 1833.4(480), 1306.5(265), 389.7(26 × 2), 256.8(52 × 2), 225.5(0)
$ZnZnH_2$[a]	ZnH: 1.544	$ZnZnH_2$: 1919.6(b_2,280), 1907.9(a_1,4), 632.9(b_1,116), 620.9(a_1,324), 164.4(b_2,4), 36.2(a_1,1).
(C_{2v})	HZnH: 176.2	
	ZnZn′: 3.301	
ZnH_4 (D_{4h})	ZnH: 1.528	ZnH_4: 1929.3(b_{3g},0), 1919.4(b_{1u},118), 1919.3(b_{2u},118), 1830.3(a_g,0), 798.7(a_u,0),
	HZnH: 89.9 and 90.1	621.2(a_g,0), 599.3(b_{3u},57), 58.1(b_{2u},104), 36.3(b_{1u},105).
Zn_2H_4 (D_{2h})	ZnH: 1.537	Zn_2H_4: 1945.5(a_g,0), 1938.5(b_{1u},245), 1480.1(a_g,0), 1213.3(b_{2u},315), 1158.3(b_{1u},838),
	ZnH′: 1.756	1156.2(b_{3g},0), 707.1(b_{3u},176), 475.7(b_{2u},109), 421.0(b_{2g},0), 286.5(b_{3u},79), 230.7(a_g,0), 164.2(b_{3g},0).
	ZnH′Zn: 89.6	

[a] Isomer 2 kcal/mol lower than linear structure.

TABLE 6: Calculated Geometries, Vibrational Frequencies, and Intensities of Cadmium Hydrides at the B3LYP/6-311++G(3df,3pd)/SDD Level of Theory

species	structure: Å	frequencies: cm^{-1}(intensities, km/mol)
CdH ($^2\Sigma$)	CdH: 1.788	CdH: 1366.1(161); CdD: 970.6(81)
Cd_2H ($^2\Sigma$)	CdH: 1.760	Cd_2H: 1473.2(σ,646), 191.7(π,29 × 2), 86.7(σ,0),
linear	CdCd: 2.991	Cd_2D: 1047.0(326), 136.6(15 × 2), 86.5(0)
Cd_3H ($^2A_1$)	CdH: 1.757	Cd_3H: 1484.0(a_1,375), 182.4(b_2,0), 177.9(b_1,42), 65.5(a_1,0), 51.6(b_2,0), 14.5(a_1,0).
C_{2V}	CdCd′: 3.083	
	Cd′CdCd′: 95.2	
Cd_4H	CdH: 1.747	Cd_4H: 1497.8(a_1,375), 205.2(e,6 × 2), 72.1(a_1,0), 44.3(e,0 × 2), 24.4(e,0 × 2), 18.5(a_1,0)
(C_{3v})	ZnZn′: 3.118	
	Zn′Zn′: 3.594	
CdH_2 ($^1\Sigma_g^+$)	CdH: 1.679	CdH_2: 1825.8(σ_g, 0), 1807.3(σ_u, 415), 646.6(π_u, 132 × 2).
linear		CdD_2: 1291.5(0), 1289.5(211), 461.3(67 × 2)
		CdHD: 1816.6(205), 1290.5(108), 562.1(100 × 2)
Cd_2H_2 ($^1\Sigma_g^+$)	CdH: 1.718	Cd_2H_2: 1670.5(σ_g,0), 1641.5(σ_u, 1281), 409.2(π_g,0 × 2), 330.1(π_u,95 × 2), 166.7(σ_g,0).
linear	CdCd: 2.715	Cd_2D_2: 1186.7(0), 1166.2(647), 295.2(0 × 2), 234.7(48 × 2), 165.9(0)
		Cd_2HD: 1656.3(618), 1176.2(346), 380.3(27 × 2), 254.5(44 × 2), 166.3(0)
Cd_2H_4 (C_{2h})	CdH: 1.673	Cd_2H_4: 1831.5(a_g,0), 1828.9(b_u,294), 1718.9(b_u,544), 1692.4(a_g,0), 722.2(a_g,0),
	CdH′: 1.706 and 2.681	640.2(a_u,216), 587.9(b_g,0), 574.3(b_u,553), 307.4(a_g,0), 187.9(a_u,97), 142.6(a_u,8), 41.5(a_g,0)
	CdH′Cd: 97.3	
Cd_3H_6 (C_{3h})	CdH: 1.682	Cd_3H_6: 1791.7(a′0), 1791.5(e′,218 × 2), 1646.6(e′,1069 × 2), 1548.9(a′,0), 713.6(a′,0),
	CdH′: 1.736 and 2.198	625.9(a″,315), 611.6(e′,459 × 2), 541.6(e″,0 × 2), 359.1(e′,37 × 2), 298.2(a′,0), 135.4(a″,23),
	CdH′Cd: 146.4	98.5(e″,0 × 2), 75.5(e′,4 × 2), 63.2(a′,0)

^{68}Zn, 18.8%) and two minor (^{67}Zn, 4.1%, ^{70}Zn, 0.6%), contribute to the higher-resolution (0.13 cm^{-1}) spectra. The strong 5/3/2 triplet is characteristic of zinc, and the zinc spectra also show the weaker, intermediate $^{67}ZnH_2$ peak and the $^{67}ZnD_2$ and $^{70}ZnD_2$ absorptions. The major frequency shifts from $^{64}ZnH_2$ for $^{66}ZnH_2$ and $^{68}ZnH_2$ are calculated in the harmonic approximation to be 0.87 and 1.69 cm^{-1}, and our observed splittings are 0.82 and 1.60 cm^{-1}, respectively. The very small differences are due to anharmonicity in the observed values. Likewise the computed splittings from $^{64}ZnD_2$ for $^{66}ZnD_2$ and $^{68}ZnD_2$ are 1.22 and 2.38 cm^{-1}, and our observed splittings are 1.18 and 2.29 cm^{-1}, respectively.

The natural cadmium isotopic distribution is dominated by ^{112}Cd(24.1%) and ^{114}Cd (28.7%).[23] The sharp major peak separation observed for CdH_2 is 0.25 cm^{-1} in *p*-H_2 and for CdD_2 in *o*-D_2 is 0.36 cm^{-1}. The calculated 112−114 cadmium splittings are 0.27 and 0.39 cm^{-1} for harmonic antisymmetric vibrations in linear isotopic molecules.

Figure 9 shows splittings for both stretching modes of ZnHD and the antisymmetric stretching mode of ZnD_2 in solid HD and provides a textbook example of isotopic mass shifts in different vibrational modes. The splittings for ZnH_2 are masked, but the peak positions from *p*-H_2 spectra are given. Notice the larger (1.19, 1.11 cm^{-1}) separations in the major components for the antisymmetric D−Zn−D stretching mode (which involves more zinc motion) than for the symmetric DZn−H vibration (0.42, 0.40 cm^{-1}) and the symmetric HZn−D mode (0.59, 0.54 cm^{-1}). The observed splittings are in excellent agreement with computed B3LYP values (0.45, 0.42 cm^{-1} and 0.60, 0.55 cm^{-1}, respectively). The zinc isotopic splitting is, of course, larger when zinc vibrates with D as opposed to H.

The ZnH_2 and CdH_2 molecules are captured here by solid molecular hydrogen matrix environments, and a new associated hydrogen ligand vibration is observed to increase with the ZnH_2 and CdH_2 fundamentals on UV irradiation. These new absorptions in both $J = 0$ and $J = 1$ modifications (for para and ortho

hydrogen ligands) are given in Tables 1 and 2. Notice that the red-shift from induced *p*-H_2 (4152.8 cm^{-1}) and *o*-H_2 (4146.7 cm^{-1}) values in hydrogen[17,21] to 4143.1 cm^{-1} for $(p\text{-}H_2)_nZnH_2$ and to 4133.6 cm^{-1} for $(o\text{-}H_2)_nZnH_2$ is slightly less for $(o\text{-}H_2)_n$-CdH_2 at 4134.0 cm^{-1}. The (o-D_2) values reveal a smaller shift from 2986.8 cm^{-1} for *o*-D_2 in solid deuterium[18,21] for CdD_2 (2977.7 cm^{-1}) than ZnD_2 (2977.2 cm^{-1}) complexes with *o*-D_2. The HD frequency is more straightforward as there is only one ($J = 0$) isomer to interpret. In solid HD, the induced HD fundamental[18,21] is 3624.7 cm^{-1}, and interaction with ZnHD shifts this to 3614.8 cm^{-1}, or CdHD affects a smaller displacement to 3615.0 cm^{-1}. The bottom line is that complexing H_2 interacts weakly with ZnH_2 and CdH_2, producing 13.1 and 12.7 cm^{-1} shifts, respectively, for *o*-H_2 and 9.9 and 9.7 cm^{-1} shifts for HD in the ligand stretching fundamental. As can be seen the H_2 ligand interaction with ZnH_2 is slightly greater than with CdH_2.

Finally, the blue satellite peak at 1887.0 cm^{-1} above ZnH_2 at 1875.5 cm^{-1} is clearly due to a perturbed ZnH_2 vibration. What then is the origin of the perturbation? We considered the ZnH_4 species, which is higher energy than $ZnH_2 + H_2$, is a local minimum energy species, and has a computed ZnH_2 mode 10 cm^{-1} lower; this was rejected. The perturbation by Zn in the $Zn-ZnH_2$ species leads to a slightly lower energy than Zn_2H_2 and a ZnH_2 mode that is also 10 cm^{-1} lower. Such a species may give rise to the satellite feature as the absolute frequency accuracy in the calculation is much greater than 20 cm^{-1}, but we cannot be certain. The satellite feature is clearly due to an $(X)ZnH_2$ species.

ZnH and CdH. The ZnH and CdH molecules give sharp bands at 1495.4 and 1340.0 cm^{-1} in the *n*-H_2 samples, which are 1.5 and 1.0 cm^{-1} higher, respectively, than solid argon values. These bands are slightly higher in *p*-H_2 or neon and very near the gas-phase values.[24−26] Again, isotopic data verifies the molecular identification. The HD experiments give single bands, which are almost identical to the solid H_2 and D_2 values (solid HD is a different medium). Although the zinc isotopic splittings are not completely resolved for ZnH and ZnD, the 5/3/2 profile is characteristic of a single Zn atom vibration.

The Zn and Cd reactions with H_2 are calculated to be endothermic,[7] and they proceed on activation by electronic excitation of Zn and Cd in either ^3P or ^1P states.[27,28] The ZnH_2 and CdH_2 molecules are for the most part relaxed and captured by the matrix, but some decomposition of the excited dihydride intermediates to ZnH and CdH does occur.

$$Zn\ (^3P, {}^1P) + H_2 \rightarrow [ZnH_2]^* \xrightarrow{\text{relax}} ZnH_2 \qquad (1a)$$

$$Cd\ (^3P, {}^1P) + H_2 \rightarrow [CdH_2]^* \xrightarrow{\text{relax}} CdH_2 \qquad (1b)$$

$$[ZnH_2]^* \rightarrow ZnH + H \qquad (2a)$$

$$[CdH_2]^* \rightarrow CdH + H \qquad (2b)$$

Zn_2H_2 and Cd_2H_2. The linear HZnZnH molecule was identified in the argon matrix investigation, and MP2 calculations found the rhombic ring structure to be 0.29 eV higher in energy.[7] Again, isotopic data confirms this assignment. The zinc isotopic splittings are not completely resolved (Figures 7, 8), but a clearly different pattern is observed with separations of about half of that for a single zinc atom. The observed splittings are in accord with that expected for two equivalent zinc atoms with the 64−68 and 66−66 isotopic pairs contributing to the central band peak.

The HD spectra show that two hydrogens are involved as both Zn−H and Zn−D stretching modes are observed. However, in contrast to ZnHD, the Zn−H mode for Zn_2HD is higher than the antisymmetric mode observed for Zn_2H_2, and the Zn−D mode for Zn_2HD is also higher than that of the observed Zn_2D_2 absorption. This happens because the symmetric Zn−H mode is higher than the antisymmetric Zn−H mode for the Zn_2H_2 molecule. Our B3LYP calculations predict the unobserved symmetric mode for Zn_2H_2 to be 25 cm^{-1} higher than the antisymmetric mode (calculated 1820.6 cm^{-1}, observed 1746.8 cm^{-1}) and, accordingly, the Zn−H mode of Zn_2HD to be 12.8 cm^{-1} higher than the observed Zn_2H_2 band. In fact, we observe the latter is 13.5 cm^{-1} higher than the former. Likewise the Zn−D mode of Zn_2HD is predicted to be 8.7 cm^{-1} higher than the antisymmetric ZnD_2 mode, and we observe it to be 9.1 cm^{-1} higher.

The HCdCdH molecule was not observed in the argon matrix investigation, but the higher CdH yield in pure hydrogen made possible the observation of its dimer. A very weak band at 1621.8 cm^{-1} on deposition increased slightly on $\lambda > 470$ nm irradiation and disappeared with UV photolysis but was restored with even more intensity on annealing, behavior shared by the 1746.8 cm^{-1} HZnZnH absorption. In deuterium, a counterpart was found at 1166.5 cm^{-1} (H/D = 1.390). The compelling evidence is found with HD, where new counterpart bands dominated at 1629.0 and 1170.9 cm^{-1}. This indicates approximately 7 and 4 cm^{-1} blue-shifts for the stretching modes of the mixed isotopic molecule relative to the all-hydrogen and -deuterium counterparts.

$$ZnH + ZnH \rightarrow HZnZnH \qquad (3a)$$

$$CdH + CdH \rightarrow HCdCdH \qquad (3b)$$

Our B3LYP calculations predict a linear, centrosymmetric HCdCdH molecule, analogous to HZnZnH, and a very strong antisymmetric stretching mode at 1641.5 cm^{-1}, in excellent agreement with the observed 1621.8 cm^{-1} absorption. Furthermore, the stretching modes for Cd_2HD are predicted to be 15 and 10 cm^{-1} above the strong bands for Cd_2H_2 and Cd_2D_2, which are in very good agreement with the above observed differences.

Zn_xH and Cd_xH. Several absorptions appear to be due to metal cluster hydrides. The 1647.9 cm^{-1} absorption and ZnH band increase 25% on $\lambda > 470$ nm irradiation (Figure 1a,b), but both are nearly destroyed by $\lambda > 360$ nm irradiation. Although ZnH reappears with UV irradiation, the 1647.9 cm^{-1} absorption requires annealing and becomes even stronger than in the initial sample deposit. A satellite absorption also appears at 1680.8 cm^{-1} on 6.3 K annealing, which increases at the expense of the 1647.9 cm^{-1} band on 7.0 K annealing while another satellite appears at 1697.2 cm^{-1}. Deuterium counterparts for the stronger first two absorptions at 1194.4 and 1214.0 cm^{-1} (and H/D ratios 1.380 and 1.385) characterize Zn−H(D) stretching modes. The HD experiment provides bands at 1649.4 and 1194.7 cm^{-1} with analogous behavior. These small changes from solid H_2 and D_2 values are due to the medium, and a single H(D) atom vibration is evidenced.

A strong 1657.6 cm^{-1} absorption in the argon matrix investigation was assigned to the ZnZnH radical on the basis of Zn concentration and H/D isotopic behavior, and the present observations are in agreement with a like assignment for the 1647.9 cm^{-1} hydrogen matrix absorption. Our B3LYP calculation for the ZnZnH structure is in good agreement with previous MP2 results,[7] and our computed Zn−H frequency (1685 cm^{-1}) is much closer to the observed value. The small red-shift from

argon to hydrogen environments indicates a weak interaction between the open-shell ZnZnH species and the hydrogen matrix. Our neon matrix counterpart at 1647.8 cm^{-1} has a 1656.4 cm^{-1} satellite much closer to the argon matrix value. Finally, we note that the analogous MgMgH radical has been characterized in similar experiments.[13]

We suggest that the growth of ZnH and Zn_2H on $\lambda > 470$ nm irradiation is due to diffusion and reaction of H atoms with Zn and Zn_2. In fact, the 4143.4 cm^{-1} absorption attributed to a hydrogen atom complex[21] is reduced by half on $\lambda > 470$ nm photolysis. The Zn_2 molecule has been formed on deposition of Zn atoms and identified by UV absorption spectra.[29] Previous workers have formed ZnH and CdH by reaction of the atoms in a matrix environment.[30] We also observe ZnH and CdH to increase on annealing the solid matrix samples.

The 1680.8 cm^{-1} band that appears on annealing behaves like a higher-order version of Zn_2H as does the weaker 1697.2 cm^{-1} absorption. The 1680.8 cm^{-1} band shifts to 1214.0 cm^{-1} in solid deuterium, and counterparts at 1681.4 and 1215.7 cm^{-1} in solid HD argue again for the vibration of a single H(D) atom. Our B3LYP calculations for Zn_3H find a stable Zn_3 triangle with terminal H and Zn−H frequency (1701 cm^{-1}) above Zn_2H. For Zn_4H, we compute a stable Zn_4 tetrahedron with terminal H and Zn−H frequency (1739 cm^{-1}) that is still higher. Accordingly, the 1680.8 and 1697.2 cm^{-1} bands are assigned to the higher Zn_3H and Zn_4H cluster radicals.

A 1521.0 cm^{-1} absorption in the Cd/Ar matrix work exhibited appropriate characteristics for assignment to CdCdH.[7] The present 1494.8 cm^{-1} absorption and CdH band both increase 25% on $\lambda > 470$ nm photolysis but are destroyed by $\lambda > 290$ nm photolysis. Excimer 193 nm irradiation restores CdH but produces only a trace absorption at 1494.8 cm^{-1}. However, annealing produces a strong, sharp 1494.8 cm^{-1} band and 1533.8 and 1547.2 cm^{-1} satellites. Our B3LYP calculations for the CdCdH radical using the SDD pseudopotential give a stable linear species, but the computed Cd−H frequency (1473 cm^{-1}) is lower than the observed value, which we attribute to poor quality of the calculation for cadmium metal clusters. Similar observations of weaker 1533.8 and 1547.2 bands and calculations for Cd_3H and Cd_4H support these assignments for the latter absorptions. A matrix shift from 1521.0 cm^{-1} for argon to 1493.0 cm^{-1} for neon and 1494.8 cm^{-1} for hydrogen is surprising, and this suggests that the former band may instead be due to another species, perhaps Cd_3H.

$(ZnH_2)_{2,3}$ and $(CdH_2)_{2,3}$. Weak absorptions at 1858.9 and 1741.9 cm^{-1} are produced on near UV irradiation as satellites of the strong ZnH_2 and CdH_2 absorptions. These bands are destroyed by 240−380 nm irradiation, but they return with moderate intensity on annealing at the expense of ZnH_2 and CdH_2, respectively. The zinc isotopic splittings (Figure 7) are virtually identical to that found for ZnH_2 itself. The 1858.9 and 1741.9 cm^{-1} absorptions are assigned to van der Waals dimers of ZnH_2 and CdH_2. It is noteworthy that no evidence of the D_{2h} dibridged Zn_2H_4 and Cd_2H_4 dimer structures was found. This contrasts with linear MgH_2, which formed a dibridged Mg_2H_4 dimer.[13]

DFT calculations of ZnH_2 dimer converged to a D_{2h} dibridged structure like that of Mg_2H_4, and the MP2 calculation gave the same result.[7,13] However, no absorptions were observed for a bridged Zn−H−Zn mode for ZnH_2 dimer in solid neon, hydrogen, and argon, suggesting that van der Waals dimers are favored in solid matrixes. Note that the dimerization of ZnH_2 is exothermic by only 6 kcal/mol based on B3LYP calculation, which is larger than predicted by MP2 calculation (1.7 kcal/mol).[31] Recall that the dimerization of MgH_2 is exothermic by 27 kcal/mol and of AlH_3 by 35 kcal/mol, and Mg_2H_4 and Al_2H_6 are the major products.[9,10,13] Calculations of CdH_2 dimer gave a C_{2h} structure that is very much like that of $(HgH_2)_2$,[32] and in fact, a van der Waals dimer of CdH_2 is observed here. This is in agreement with MP2 calculations, which find a C_{2h} minimum and a D_{2h} transition state for $(CdH_2)_2$, and a small 2.1 kcal/mol dimerization energy for CdH_2.[31] Our B3LYP calculation apparently overestimates the monomer interaction in the dimer as the frequency shift observed for the dimer (20.6 cm^{-1}) is smaller than calculated (88.4 cm^{-1}).

The weaker absorptions at 1842.0 and 1724.9 cm^{-1} are appropriate for the next-higher cluster, namely the van der Waals trimers. Only a broad contour was observed for the 1842.9 cm^{-1} band in solid *p*-H_2 as zinc isotopic splittings could not be resolved.

Solid Hydrides. After the hydrogen or neon matrix evaporates, the sharp absorptions above are replaced by the broad bands illustrated in Figure 6. Stronger bands are observed with pure hydrogen (D_2 or HD), owing to the higher product yield. The H/D frequency ratios (1.37 and 1.38, Table 3) are in agreement with the ZnH_2 (1.3775) and CdH_2 (1.3851) molecule values. Notice that the HD reagent gave slightly higher-frequency broad bands in each case. This indicates that the pure isotopic solids have an unobserved higher-frequency symmetric M−H stretching mode.

The thermal properties of our solid films are in general agreement with observations in several reports for solid ZnH_2 and CdH_2.[1−4,8] The former is reported to be stable up to 90−115° and the latter to −20 °C. Our solid zinc hydride spectrum was unchanged at room temperature, and our solid cadmium hydride spectrum disappeared near 250 K. Accordingly, the broad 1440 and 1340 cm^{-1} absorptions are assigned to solid ZnH_2 and CdH_2, respectively, which are formed by association of the monomers after sublimation of the matrix. It is important to note that the broad 1440 and 1340 cm^{-1} absorptions characterize solid ZnH_2 and CdH_2 as hydrogen-bridged solid polymers qualitatively like those found for solid MgH_2.[33] The broad absorptions observed at 1160 and 560 cm^{-1} for solid MgH_2 in similar hydrogen matrix experiments[13] are strikingly similar to the neutron-scattering spectrum of the authentic solid material.[34] The infrared spectrum of solid ZnH_2 has been described simply as broad 1900−1300, 1150−850, and 650−500 cm^{-1} bands.[3] Our spectrum is in agreement if the intermediate band is weaker.

HZnOH. Weak new absorptions appeared at 1963.2 cm^{-1} in *n*-H_2, 1965.8 cm^{-1} in *p*-H_2, 1415.7 cm^{-1} in *n*-D_2, and 1417.1 cm^{-1} in *o*-D_2 on UV irradiation. These bands are in excellent agreement with the 1955 cm^{-1} band reported for the Zn−H stretching mode of HZnOH in solid argon.[7] The pure HD experiment revealed new sharp absorptions at 1965.1 and 1416.7 cm^{-1} (Figure 3) plus weaker new bands at 662.7, 661.4, and 480.1 cm^{-1} for the HZnOD and DZnOH mixed isotopic species. In the three $J = 0$ solids, these bands showed resolved zinc isotopic splittings for a single Zn atom vibration. The *p*-H_2 sample gave peaks at 1965.84, 1965.38, and 1964.94 cm^{-1} for the 5/3/2 relative intensity 64, 66, 68 zinc isotopic triplet. This new information demonstrates that a single Zn atom is involved in the subject vibrational mode. The 1955 cm^{-1} band and several weaker fundamentals have recently been produced by the excited Zn atom reaction with H_2O in excess argon,[35] which confirms these HZnOH assignments.

Conclusions

Laser-ablated Zn and Cd atoms react with molecular hydrogens upon condensation at 4.5 K to form the metal dihydride molecules in solid hydrogen and neon. Ultraviolet irradiation increases these absorptions by an order of magnitude. Natural zinc and cadmium isotopic splittings are resolved in solid *p*-H_2, *o*-D_2, and HD. The antisymmetric stretching fundamental of ZnH_2 in solid neon (1880.6 cm^{-1}) and *p*-H_2 (1880.5 cm^{-1}) is just above the median of the argon matrix (1870.2 cm^{-1}) and the recently determined gas phase value (1889.4 cm^{-1}).[36] In fact, the weak (X)ZnH_2 band at 1891.1 cm^{-1} in *p*-H_2 could be due to essentially gaseous ZnH_2 in a loose cage or on the matrix surface. Weaker absorptions are assigned to the linear HMMH molecules and to metal cluster monohydrides with the assistance of DFT calculations.

Upon sublimation of the hydrogen or neon matrix, the metal dihydride molecules polymerize into solid hydrides with broad absorption bands characteristic of hydrogen-bridge bonding.

Acknowledgment. We gratefully acknowledge support from N.S.F. Grants CHE 00-78836 and CHE 03-52487.

References and Notes

(1) Barbaras, G. D.; Dillard, C.; Finholt, A. E.; Wartik, T.; Wilzbach, K. E.; Schlesinger, H. I. *J. Am. Chem. Soc.* **1951**, *73*, 4585.
(2) Wiberg, E.; Henle, W.; Bauer, R. *Z. Naturforsch.* **1951**, *6b*, 393 (Zn).
(3) De Koning, A. J.; Boersma, J.; van der Kerk, G. J. M. *J. Organomet. Chem.* **1980**, *186*, 159.
(4) Shaw, B. L. *Inorganic Hydrides*; Pergamon: Oxford, 1967.
(5) Mikhailov, Yu. I.; Maltseva, N. N.; Kedrova, N. S.; Brosalin, A. B.; Kuznetsov, N. T.; Boldyrev, V. *Inorg. Mater.* **1985**, *8*, 1329.
(6) Xiao, Z. L.; Hauge, R. H.; Margrave, J. L. *High Temp. Sci.* **1991**, *31*, 59.
(7) Greene, T. M.; Brown, E.; Andrews, L.; Downs, A. J.; Chertihin, G. V.; Runeberg, N.; Pyykkö, P. *J. Phys. Chem.* **1995**, *99*, 7925.
(8) Wiberg, E.; Henle, W. *Z. Naturforsch.* **1951**, *6b*, 461 (Cd).
(9) Andrews, L.; Wang, X. *Science* **2003**, *299*, 2049.
(10) Wang, X.; Andrews, L. Tam, S.; DeRose, M. E.; Fajardo, M. *J. Am. Chem. Soc.* **2003**, *125*, 9218 (Al+H_2).
(11) Andrews, L.; Wang, X. *Angew. Chem. Int. Ed.* **2004**, *43*, 1706.
(12) Wang, X.; Andrews, L. *J. Phys. Chem. A* **2004**, *108*, 4440 (In+H_2).
(13) Wang, X.; Andrews, L. *J. Phys. Chem. A.* **2004**. In press. (Mg+H_2).
(14) Andrews, L.; Citra, A. *Chem. Rev.* **2002**, *102*, 885 and references therein.
(15) Andrews, L. *Chem. Soc. Rev.* **2004**, *33*, 123 and references therein.
(16) Andrews, L.; Wang, X. *Rev. Sci. Instrum.* **2004,** *75***,** 3039(para hydrogen converter).
(17) Gush, H. P.; Hare, W. F.; Allin, E. J.; Welsh, H. L. *Can. J. Phys.* **1960**, *38*, 176.
(18) Crane, A.; Gush, H. P. *Can. J. Phys.* **1966**, *44*, 373.
(19) Frisch, M. J.; Trucks, G. W.; Schlegel, H. B.; Scuseria, G. E.; Robb, M. A.; Cheeseman, J. R.; Zakrzewski, V. G.; Montgomery, J. A., Jr.; Stratmann, R. E.; Burant, J. C.; Dapprich, S.; Millam, J. M.; Daniels, A. D.; Kudin, K. N.; Strain, M. C.; Farkas, O.; Tomasi, J.; Barone, V.; Cossi, M.; Cammi, R.; Mennucci, B.; Pomelli, C.; Adamo, C.; Clifford, S.; Ochterski, J.; Petersson, G. A.; Ayala, P. Y.; Cui, Q.; Morokuma, K.; Malick, D. K.; Rabuck, A. D.; Raghavachari, K.; Foresman, J. B.; Cioslowski, J.; Ortiz, J. V.; Stefanov, B. B.; Liu, G.; Liashenko, A.; Piskorz, P.; Komaromi, I.; Gomperts, R.; Martin, R. L.; Fox, D. J.; Keith, T.; Al-Laham, M. A.; Peng, C. Y.; Nanayakkara, A.; Gonzalez, C.; Challacombe, M.; Gill, P. M. W.; Johnson, B.; Chen, W.; Wong, M. W.; Andres, J. L.; Gonzalez, C.; Head-Gordon, M.; Replogle, E. S.; Pople, J. A. *Gaussian 98*, revision A.11.4, Gaussian, Inc.: Pittsburgh, PA, 1998 and references therein.
(20) Wang, X.; Andrews, L. *J. Phys. Chem. A* **2004**, *108*, 1103.
(21) Andrews, L.; Wang, X. *J. Phys. Chem. A* **2004**, *108*, 3879.
(22) Momose, T.; Shida, T. *Bull. Chem. Soc. Jpn.* **1998**, *71*, 1.
(23) *CRC Handbook, Table of the Isotopes*, 66th ed.; CRC: Boca Raton, FL, 1985.
(24) Huber, K. P.; Herzberg, G. *Spectra of Diatomic Molecules*; Van Nostrand Reinhold: New York, 1979.
(25) Urban, R.-D.; Magg, U.; Birk, H.; Jones, H. *J. Chem. Phys.* **1990**, *92*, 14.
(26) Birk, H.; Urban, R.-D.; Polomsky, P.; Jones, H. *J. Chem. Phys.* **1991**, *94*, 5435.
(27) Breckenridge, W. H.; Wang, J.-H. *J. Phys. Chem.* **1987**, *87*, 2630.
(28) Wallace, L.; Funk, D. J.; Kemp, J. G.; Breckenridge, W. H. *J. Chem. Phys.* **1992**, *97*, 3135.
(29) Ault, B. S.; Andrews, L. *J. Mol. Spectrosc.* **1977**, *65*, 102.
(30) Knight, L. B., Jr.; Weltner, W., Jr. *J. Chem. Phys.* **1971**, *55*, 2061.
(31) Kaupp, M.; von Schnering, H. G. *Inorg. Chem.* **1994**, *33*, 4718.
(32) Pyykkö, P.; Straka, M. *Phys. Chem. Chem. Phys.* **2000**, *2*, 2489.
(33) Santisteban, J. R.; Cuello, G. J.; Dawidowski, J.; Fainstein, A.; Peretti, H. A.; Ivanov, A.; Bermejo, F. J. *Phys. Rev. B* **2000**, *62*, 37.
(34) Zachariasen, W. H.; Holley, C. E.; Stampfer, J. F. *Acta Crystallogr.* **1963**, *16*, 352.
(35) Macrae, V. A.; Greene, T. M.; Downs, A. J. *Phys. Chem. Chem. Phys.* **2004**, 4586-4594.
(36) Shayesteh, A.; Appadoo, D. R. T.; Gordon, I. E.; Bernath, P. F. *J. Am. Chem. Soc.* **2004**, *126*, 14356.